Licoisoflavone A ameliorates adipose tissue dysfunction in diet-induced obesity by promoting METTL3 expression

SHUANGXI TU[1*], XIAODAN WANG[1*], ZHENBO WANG[2*], HAOJUN TANG[1], KAI YIN[2] and XIAO ZHU[1,2]

[1]Guangxi Key Laboratory of Diabetic Systems Medicine, Guilin Medical University, Guilin, Guangxi Zhuang Autonomous Region 541199, P.R. China; [2]Guangzhou Key Laboratory of Diabetes Metabolic Reprogramming and Precision Prevention and Control, Department of General Practice, The Fifth Affiliated Hospital of Southern Medical University, Guangzhou, Guangdong 510900, P.R. China

Received February 10, 2026; Accepted August 5, 2026

DOI: 10.3892/mmr.2026.14007

Abstract. With the development of obese adipose tissue (AT), adipocytes undergo pathological changes from inert energy storage to excessive and active endocrine organs associated with disease hazards. Methyltransferase 3 (METTL3) is an RNA methyltransferase with key roles in AT development, functional maintenance and metabolic homeostasis. Licoisoflavone A (LIC-A) is a prenylated flavonoid compound derived from licorice, which has anti-inflammatory, antihypertrophic and antiproliferative activities; however, whether it directly modulates METTL3 expression and affects AT function in obesity remains unknown. In the present study, molecular docking of compounds from the traditional Chinese medicine formula Fangji-Huangqi Decoction against METTL3, identified 16 top-ranked candidate molecules. Among these candidates, LIC-A was identified as a potential upstream regulator of METTL3 and markedly increased METTL3 expression. The effects of TNF-α and lipopolysaccharide treatments on the inhibition of adipogenesis were successfully recovered by LIC-A treatment of the adipogenic 3T3-L1 cells, via the regulation of adipogenic cytokines, as well as the expression of inflammatory factors. These protective effects were similarly abolished by METTL3 knockdown, suggesting that the role of LIC-A relies on METTL3. Moreover, *in vivo* data demonstrated that the administration of LIC-A could notably recover body weight lipid metabolism, insulin resistance and gluconeogenesis in mice with reduced adipose deposition, as well as abate systemic inflammation. The novelty of the present study lies in three aspects: i) LIC-A was identified as a previously unrecognized upstream positive regulator of METTL3 expression; ii) LIC-A was demonstrated to alleviate adipokine dysregulation and AT inflammation through a METTL3-dependent mechanism; and iii) the first *in vivo* experimental evidence that LIC-A can improve obesity-related metabolic disorders by promoting METTL3-mediated m6A methylation in AT was provided. To the best of our knowledge, this is the first study to link a natural isoflavone compound from licorice to METTL3-mediated post-transcriptional regulation in the context of AT dysfunction.

Correspondence to: Professor Kai Yin or Dr Xiao Zhu, Guangzhou Key Laboratory of Diabetes Metabolic Reprogramming and Precision Prevention and Control, Department of General Practice, The Fifth Affiliated Hospital of Southern Medical University, 566 Congcheng Avenue, Conghua, Guangzhou, Guangdong 510900, P.R. China
E-mail: kaiyinby@qq.com
E-mail: 1365681080@qq.com

*Contributed equally

Key words: obesity, licoisoflavone A, methyltransferase 3, adipose tissue, inflammation

Introduction

Obesity is a complex chronic metabolic disorder related to a plethora of comorbidities, such as metabolic syndrome (1), insulin resistance (2), hypertension and diabetes (3). Excessive accumulation of body fat in adipose tissue (AT) is a major feature of obesity and occurs primarily through triglyceride storage, leading to adipocyte hypertrophy and/or hyperplasia. Although AT inflammation is typically low grade, continuous stimulation by inflammatory mediators is sufficient to cause major organ dysfunction and lead to the onset of metabolic obesity-derived complications (4,5). Synthetic anti-obesity agents currently available include orlistat, an anti-obesity agent that inhibits gastrointestinal and pancreatic lipases, thereby decreasing intestinal fat absorption (6), and liraglutide, an agent that preferentially decreases fat mass but increases lean body mass (7,8). Pharmacological interventions represent an increasingly promising avenue for the treatment of obesity. However, adverse drug reactions remain a notable public health concern and a major barrier to anti-obesity drug development. Notable examples include the serious adverse events associated with naltrexone/bupropion (such as cardiovascular events, seizures, severe psychiatric symptoms including suicidal ideation, hepatotoxicity and severe hypersensitivity) and the dose-dependent gastrointestinal events (nausea, vomiting and diarrhea) frequently observed with semaglutide (9,10). Consequently, identifying specific molecular targets that regulate adipose tissue function and developing targeted therapies are of considerable relevance.

Methyltransferase 3 (METTL3) serves as the core catalytic subunit of the m^6A methyltransferase complex (11-13) and plays a central role in numerous biological processes, including cell proliferation, migration (14,15) and energy metabolism (16-18). As the most abundant reversible chemical modification in eukaryotic mRNA (19,20), m^6A methylation is dynamically regulated by 'writer' (for example METTL3) (21,22), 'eraser' (for example fat mass and obesity-associated protein) (23) and 'reader' proteins (for example YTH domain family proteins 1/2/3) (24-26), which collectively modulate mRNA processing and fate (27,28). A previous study has demonstrated that METTL3-mediated m^6A modification promotes the induction of beige adipocytes within white AT (WAT), a process associated with improved glucose and lipid metabolism and protection against obesity (29). Moreover, METTL3 upregulates glycolytic genes via m^6A modification during cold-induced activation of beige adipocytes (30). These findings highlight the potential of targeting METTL3-mediated m^6A modification to restore AT homeostasis.

Traditional Chinese medicine (TCM) has emerged as a promising source of anti-obesity agents, with accumulating evidence highlighting the therapeutic potential of herbal formulations in modulating energy homeostasis and AT function (31,32). Given their structural diversity and potential for multitarget modulation, natural products warrant continued exploration as sources of anti-obesity lead compounds. Among these, Fangji-Huangqi Decoction (FJHQT), a classic formula originally documented in Zhang Zhongjing's Jin Gui Yao Lue (Synopsis of the Golden Chamber), has garnered particular interest for its anti-obesity properties (33,34). FJHQT comprises four medicinal herbs, Stephaniae tetrandrae Radix (Fangji), Astragali Radix (Huangqi), Atractylodis macrocephalae Rhizoma (Baizhu) and Glycyrrhizae Radix (Gancao), and has been reported to enhance glucose and lipid metabolism and induce considerable weight loss, representing one of the earliest TCM formulas with recognized anti-obesity efficacy that has gained international attention (35-37). A growing body of evidence supports the anti-obesity effects of FJHQT and its constituent herbs. FJHQT is identified as a TCM therapy that affects appetite-regulating pathways, primarily by regulating the hypothalamic AgRP/NPY and POMC/CART neuropeptide systems and the leptin signaling pathway (33). Notably, each component of FJHQT independently exhibits anti-obesity or metabolic regulatory effects. Fangji and its alkaloid tetrandrine have shown anti-obesity potential by reducing leptin expression and inhibiting adipogenesis through downregulation of CCAAT/enhancer-binding protein α and peroxisome proliferator-activated receptor-γ (38). Huangqi is highly relevant to lipid metabolism and lipolysis pathways, and is widely reported to improve insulin resistance and dyslipidemia (39,40). Baizhu, in combination with other herbs, is reported to improve high-fat diet (HFD)-induced obesity by suppressing adipogenesis (41). Gancao and its flavonoids reduce obesity and restore metabolic homeostasis by inducing AT browning and suppressing lipogenesis (42,43). Based on this body of evidence, FJHQT has been established as a rationally designed TCM formula whose anti-obesity effects are well supported by the literature, making it an ideal source for identifying bioactive compounds that regulate METTL3 expression and AT function. However, the specific active components of FJHQT that mediate its metabolic benefits, as well as the underlying molecular mechanisms, remain largely unknown.

Therefore, we hypothesized that FJHQT contains bioactive compounds capable of regulating METTL3 expression and ameliorating AT dysfunction. Identifying such compounds may suggest new therapeutic approaches to obesity-associated metabolic syndrome. Based on the molecular docking screening of compounds from the four herbal ingredients of FJHQT, Licoisoflavone A (LIC-A) , a principal natural isoflavone in Glycyrrhizae Radix (Gancao, one of the four constituent herbs of FJHQT), was identified as a top-ranked candidate. To the best of our knowledge, its role in obesity has not previously been investigated. Accordingly, in the present study, the effects of LIC-A on adipokine secretion and inflammatory responses in TNF-α or LPS stimulated 3T3-L1 adipocytes were evaluated, and its metabolic effects assessed in a high-fat diet (HFD)-induced obese mouse model.

Materials and methods

Animal experiments. The animal study was conducted according to a protocol approved by the Institutional Animal Care and Use Committee of Guilin Medical University, Guilin, China (approval no. IACUC-202510137) and adhered to the National Institutes of Health guidelines for laboratory animal welfare. A total of 12 male C57BL/6J mice (aged 4 weeks; body weight 12-15 g at arrival) were obtained from Cyagen Biosciences, Inc. Male mice were selected to minimize the potential confounding effects of estrous cycle-associated hormonal fluctuations on metabolic parameters, including body weight, insulin sensitivity and AT inflammation, thereby ensuring more stable and reproducible readouts for the assessment of LIC-A efficacy. The experimental mice were housed under standard specific-pathogen-free conditions, with a 12 h light-dark cycle, at a temperature of 24±2˚C and a humidity of 50±10˚C, and were allowed *ad libitum* access to a HFD (manufactured by Biotech HD Biotechnology Co., Ltd.). This purified diet was specifically formulated for diet-induced obesity studies with the following approximate composition: 34.9% fat (primarily lard), 23.5% protein (casein) and 26.2% carbohydrates (maltodextrin and sucrose), providing 60% of the total calories from fat, 20% from protein and 20% from carbohydrates, with an energy density of 5.24 kcal/g.

Throughout the experimental period, all mice were monitored daily for general health status, behavioral changes and body weight. To minimize animal suffering and ensure compliance with ethical guidelines, the following humane endpoints were predefined in accordance with the IACUC-approved protocol (approval no. GLMU-IACUC-202510137): i) Body weight loss exceeding 20% of baseline body weight (measured at the start of dietary intervention); ii) persistent clinical signs of severe illness or distress lasting >48 h, including but not limited to hunched posture, piloerection, lethargy, immobility or markedly reduced responsiveness to external stimuli; iii) severe neurological symptoms (for example convulsions, circling behavior and/or paralysis) or persistent respiratory distress (for example labored breathing and/or cyanosis) that did not resolve spontaneously within 2 h; and iv) severe abdominal distension or ulcerative dermatitis that interfered with normal movement or caused visible bleeding. Animals meeting any

of these criteria would be immediately euthanized under deep anesthesia (sodium pentobarbital, 100 mg/kg, intraperitoneal injection) prior to the scheduled endpoint to prevent unnecessary suffering. During the entire study, no animals in either the control group or the LIC-A treatment group reached any of these predefined humane endpoints, confirming that the experimental interventions were well tolerated. All animals were therefore maintained until the scheduled termination at week 16, at which point they were euthanized for tissue collection as described below.

At week 4 after the start of the HFD intervention, the mice were randomly divided into two groups (n=6 per group): i) Control group (0.5% carboxymethyl cellulose sodium by oral gavage); and ii) LIC-A treatment group (60 mg/kg body weight LIC-A dissolved in 0.5% carboxymethyl cellulose sodium by oral gavage). From week 4 to 16 after the start of the dietary intervention, treatment was administered twice weekly (for a total of 24 doses). Body weight was recorded weekly. At week 15, metabolic assessments including glucose tolerance tests (GTT) and insulin tolerance tests (ITT) were performed with a 3-day recovery interval between tests. After the metabolic assessments, the mice were allowed to recover and continued to receive the respective treatments until the end of week 16. At the end of week 16, mice were deeply anesthetized by intraperitoneal injection of 1% sodium pentobarbital (50 mg/kg body weight). Blood was collected from the retro-orbital venous plexus using a heparinized glass capillary tube (inner diameter 0.9-1.0 mm) and immediately transferred to a sterile tube without anticoagulant. In total, 0.6-0.8 ml of blood was obtained and after blood collection, gentle pressure was applied to the orbit to ensure hemostasis. Mice were then euthanized by cervical dislocation while still under deep anesthesia. The blood samples were allowed to clot at room temperature for 30 min and subsequently centrifuged at 1,500 x g for 15 min at 4˚C. The resulting serum supernatant was carefully aspirated, aliquoted and stored at -80˚C for subsequent biochemical and ELISA analyses. Epididymal WAT (eWAT) and inguinal WAT (iWAT) were rapidly dissected and collected for subsequent analysis.

Molecular docking. To identify potential upstream regulators of METTL3 in FJHQT, a multistep virtual screening strategy was employed. First, using the Traditional Chinese Medicine Systems Pharmacology Database and Analysis Platform (TCMSP), compounds were screened from the chemical constituents of four herbal ingredients: Stephaniae Tetrandrae Radix (Fangji), Astragali Radix (Huangqi), Atractylodis macrocephalae Rhizoma (Baizhu) and Glycyrrhizae Radix (Gancao), to construct a compound library. The initial library comprised 528 compounds.

Second, to identify compounds with favorable pharmacokinetic properties and drug-like characteristics, the compound library was screened using Lipinski's rule of five, which comprises four criteria related to oral bioavailability: Molecular weight <500 Da, ≤5 hydrogen bond donors, ≤10 hydrogen bond acceptors and a calculated logP value <5. Compounds that did not meet any of these criteria were excluded. This step ensured that the selected compounds possessed sufficient oral absorption and bioavailability to meet the requirements for subsequent *in vivo* evaluation.

Third, the three-dimensional (3D) structure of METTL3 was retrieved from the Protein Data Bank (PDB; https://www.rcsb.org; PDB ID: 5TEY) and processed using Discovery Studio 2021 software (Dassault Systèmes Americas Corp.). The binding pocket was defined within a 5 Å radius around the native ligand. Flexible docking analysis was performed using the LibDock module and the ligand-protein binding affinities were ranked based on LibDock score values. Ultimately, the 16 compounds with the highest docking scores were selected for further experimental validation (Table SI). LIC-A exhibited the strongest METTL3 expression-promoting activity in the subsequent experiments.

Cell culture. 3T3-L1 cells (Wuhan Pricella Biotechnology Co., Ltd.) were maintained in DMEM (Beijing Solarbio Science & Technology Co., Ltd.) supplemented with 10% heat-inactivated fetal bovine serum (FBS: Sangon Biotech Co., Ltd.) and 1% penicillin-streptomycin (MilliporeSigma) at 37˚C in a humidified atmosphere containing 5% CO_2.

For experimental assays, 3T3-L1 cells were seeded at the following densities: i) $5x10^3$ cells/well in 96-well plates; ii) $2x10^5$ cells/well in 6-well plates; and iii) $1x10^6$ cells per T25 flask. The cells were allowed to adhere overnight prior to treatment.

Cocktail induction method. To induce adipogenic differentiation, 3T3-L1 cells were cultured in T25 flasks or 6-well plates at 37˚C in a humidified atmosphere with 5% CO_2 until they reached 100% confluency. The standard medium was then replaced with adipogenic differentiation medium supplemented with 0.5 mM 3-isobutyl-1-methylxanthine (IBMX; Beijing Solarbio Science & Technology Co., Ltd.), 1 μM dexamethasone (Beyotime Biotechnology) and 1 μg/ml insulin (Wuhan Pricella Biotechnology Co., Ltd.), and the cells were incubated under the same conditions. After 3 days of induction, the medium was switched to maintenance medium (DMEM containing 10% FBS and 1 μg/ml insulin). Subsequently, the maintenance medium was refreshed every 2 days until day 8 to support complete differentiation.

After differentiation, 3T3-L1 adipocytes were treated in the presence or absence of TNF-α (10 ng/ml; Wuhan Pricella Biotechnology Co., Ltd.) or LPS (100 ng/ml; Wuhan Pricella Biotechnology Co., Ltd.), with or without LIC-A (Beijing Kangrun Chengye Biotechnology Co., Ltd.). Based on the optimal concentrations determined by MTT assay, LIC-A was used at 8 μmol/l for TNF-α-stimulated experiments and 6 μmol/l for LPS-stimulated experiments. Cells were pretreated with LIC-A for 6 h, followed by 24 h of co-culture with TNF-α or LPS. The control group was treated with an equal volume of vehicle (0.1% DMSO, the solvent for LIC-A) and maintained under the same culture conditions without any drug exposure. The experimental groups included: i) Control group; ii) group treated with LIC-A alone; iii) group treated with TNF-α alone; iv) group treated with LPS alone; v) group treated with the combination of TNF-α and LIC-A; and vi) group treated with the combination of LPS and LIC-A. In the METTL3 knockdown experiment, cells transduced with short hairpin (sh) METTL3 were subjected to the same treatment protocol and compared with the sh negative control (NC) group. Each experiment was performed at least three times to ensure reproducibility.

MTT detection of cell viability. Cells were treated with 5 mg/ml MTT solution (MedChemExpress; cat. no. HY-15924) and incubated for 4 h at 37˚C. After removing the supernatant, the resulting formazan crystals were solubilized by adding DMSO and agitating the plates for 10 min. The optical density (OD) of each well was subsequently measured at 490 nm using a microplate reader.

RNA extraction and quantification. Total RNA was extracted from cultured 3T3-L1 or AT cells using the TRIzol reagent (Invitrogen; Thermo Fisher Scientific, Inc.) according to the manufacturer's instructions. After extraction, the RNA concentration and purity were determined using a multifunctional microplate reader (BioTek; Agilent Technologies, Inc.), and the RNA purity was assessed by calculating the absorbance ratios, A260/A280 and A260/A230. Only samples with an A260/A280 ratio between 1.8 and 2.0 and an A260/A230 ratio >2.0 were selected as purified samples for subsequent experiments. The RNA concentration was then adjusted to 1 μg/μl using RNase-free water and the samples were stored at -80˚C until use.

RNA m^{6}A quantitative assay. Total RNA was extracted and quantified as described in the RNA extraction and quantification subsection. Relative m6A levels in total RNA were measured using an m^{6}A RNA Methylation Quantification Kit (Wuhan Aimeijie Technology Co., Ltd.; cat. no. P-9008-48) according to the manufacturer's instructions. For the assay, 200 ng of extracted RNA was added to each well and incubated in the provided binding solution at 37˚C for 90 min to facilitate RNA immobilization. Following the washing steps, the captured RNA was incubated sequentially with capture and detection antibodies. Colorimetric signals were developed and quantified by measuring the OD at 450 nm. Each reaction was performed in triplicate to calculate relative m^{6}A levels.

m^{6}A dot blot assays. The total RNA was harvested as described in the RNA extraction and quantification subsection. Equal amounts of total RNA (concentration determined by spectrophotometry) were heat-denatured at 95˚C for 10 min and then snap-cooled on ice. Samples were blotted onto an N+ nylon membrane. The RNA was immobilized by UV cross-linking. The membrane was blocked with 5% (w/v) non-fat dry milk in PBST [phosphate-buffered saline containing 0.1% (v/v) Tween-20] for 1 h at room temperature, followed by overnight incubation at 4˚C with a primary antibody against m^{6}A (1:2,000; Proteintech Group, Inc.; cat. no. 68055-1-Ig). After extensive washing with PBST, the membrane was probed with a horseradish peroxidase (HRP)-conjugated goat anti-rabbit IgG secondary antibody (1:5,000; Proteintech Group, Inc.; cat. no. RGAR001-50ul)) for 1 h at room temperature on a shaker. Signals were developed using an enhanced chemiluminescence (ECL) kit (Shanghai Epizyme Biomedical Technology Co., Ltd.; cat. no. SQ201) and captured using a chemiluminescence imaging system.

ELISA for IL-6, IL-1β, adiponectin, resistin and leptin. The levels of inflammatory cytokines (IL-6 and IL-1β) and adipokines (adiponectin, resistin and leptin) secreted into the culture medium by 3T3-L1 cells following LIC-A treatment were determined by ELISA. The following ELISA kits were purchased from Wuhan Elabscience Biotechnology Co., Ltd.: IL-6 (cat. no. E-AB-F1207D), IL-1β (cat. no. E-EL-M0037), leptin (cat. no. E-EL-M3008-96T), adiponectin (cat. no. E-EL-M0002-96T) and resistin (cat. no. E-EL-M3056-96T). The assays were performed strictly following the manufacturer's instructions and the OD was measured at 450 nm on a microplate reader. All measurements were performed in triplicate for each sample.

Reverse transcription-quantitative polymerase chain reaction (RT-qPCR). Total RNA was extracted from 3T3-L1 cells or AT and quantified as described in the RNA extraction and quantification subsection. RT was performed using PrimeScript II RT Mix with gDNA Remover (Beijing Kangrun Chengye Biotechnology Co., Ltd.; cat. no. A224) according to the manufacturer's instructions. Briefly, 1 μg of total RNA was mixed with 2 μl of 5X gDNA Remover Reaction buffer and 1 μl of gDNA Remover in DEPC-treated water (total volume 10 μl), then incubated at 37˚C for 5 min to remove genomic DNA. Subsequently, 10 μl of the gDNA-removed RNA sample was added to a mixture containing 4 μl of 5X RT Reaction Mix, 1 μl of PrimeScript II RT and DEPC-treated water to a final volume of 20 μl. The RT reaction was carried out at 42˚C for 15 min, followed by inactivation at 85˚C for 5 min. The resulting cDNA was placed on ice for immediate use or stored at -20˚C for subsequent experiments.

Following RT, the resulting cDNA was subjected to qPCR with 2X Taq PCR Master Mix (Wuhan Huarui Kang Biotechnology Co., Ltd.) using a real-time PCR system (Thermo Fisher Scientific, Inc.). The thermal cycling program was as follows: Initial denaturation at 95˚C for 3 min, followed by 40 cycles of denaturation at 95˚C for 15 sec, annealing at 54˚C for 30 sec and extension at 72˚C for 30 sec. To verify amplification specificity, melting curve analysis was performed from 65˚C to 95˚C in 0.5˚C increments. Gene expression levels were normalized to β-actin and calculated using the $2^{-\Delta\Delta Cq}$ method (44). Primer sequences and their corresponding annealing temperatures are listed in Table SII.

Western blotting. Total protein was extracted from 3T3-L1 cells or AT using precooled RIPA lysis buffer (Beijing Solarbio Science & Technology Co., Ltd.) supplemented with a 1% protease inhibitor cocktail (MilliporeSigma). After centrifugation at 12,000 x g for 15 min at 4˚C, the supernatant was collected. Protein concentration was determined using a BCA protein assay kit (Beyotime Biotechnology) according to the manufacturer's instructions. Briefly, the working reagent was prepared by mixing solutions A and B at a 50:1 ratio (v/v). A 25 μl aliquot of either the bovine serum albumin (BSA) standard or the diluted protein sample (the original sample was diluted 10-fold with ultrapure water) was added to individual wells of a 96-well plate. Subsequently, 200 μl of the working reagent was added to each well and the plate was incubated at 37˚C for 30 min with gentle shaking. The absorbance was measured at 562 nm using a microplate reader. Following quantification, equal aliquots of protein (25-30 μg per lane) were resolved by 10% sodium dodecyl sulfate-polyacrylamide gel electrophoresis and electrotransferred onto 0.45 μm PVDF membranes

(Merck KGaA). The membranes were blocked with 5% non-fat milk in Tris-buffered saline containing 0.1% (v/v) Tween-20 (TBST) for 2 h at room temperature and then probed overnight at 4˚C with primary antibodies targeting METTL3 (1:10,000; Proteintech Group, Inc.; cat. no. 15073-1-AP), monocyte chemoattractant protein-1 (1:2,000; Proteintech Group, Inc.; cat. no. HZ-1334), IL-6 (1:2,000; Proteintech Group, Inc.; cat. no. 83747-5-RR) and β-actin (1:5,000; Proteintech Group, Inc.; cat. no. 66009-1-Ig). After extensive washing with TBST, the membranes were incubated with appropriate HRP-conjugated secondary antibodies (goat anti-mouse or goat anti-rabbit IgG; 1:4,000; OriGene Technologies, Inc.) for 2 h at 4˚C. Immunoreactive bands were detected using an ECL substrate (Shanghai Epizyme Biomedical Technology Co., Ltd.; cat. no. SQ201) and imaged using a Tanon-5200SF chemiluminescence imaging system (Tanon Science and Technology Co., Ltd.). Densitometric analysis was performed using the Tanon-5200SF system software (version ALLDOC; Tanon Science & Technology Co., Ltd.).

Immunofluorescence. Mouse AT samples were fixed with 4% paraformaldehyde at 4˚C for 2 h, dehydrated, embedded in paraffin and cut into 7 μm-thick sections. The sections were deparaffinized, rehydrated and then permeabilized with 0.5% Triton X-100 in PBS and blocked overnight with 2% BSA in PBS at 4˚C. The tissues were then incubated overnight at 4˚C with primary antibodies against METTL3 (1:200; Proteintech Group, Inc.; cat. no. 15073-1-AP), F4/80 (1:200; Proteintech Group, Inc.; cat. no. 28463-1-AP) and Plin1 (1:300; Proteintech Group, Inc.; cat. no. 83905-4-RR). After washing, the sections were incubated with fluorophore-conjugated secondary antibodies for 1 h at room temperature as follows: Cy3-conjugated goat anti-rabbit IgG (1:400; Proteintech Group, Inc.) for METTL3, Cy3-conjugated goat anti-rabbit IgG (1:400; Proteintech Group, Inc.) for F4/80 and FITC-conjugated goat anti-rabbit IgG (1:400; Proteintech Group, Inc.) for Plin1. Nuclei were counterstained with a DAPI-containing antifade mounting medium (Beijing Solarbio Science & Technology Co., Ltd.) at room temperature for 5 min. Fluorescent images were acquired using a confocal microscope.

Lentiviral transduction. Three independent shRNA sequences targeting mouse METTL3 (NM_019721; CDS region 138-1,880 bp) were designed and inserted into the GV493 lentiviral vector (Shanghai GeneChem Co., Ltd.). The resulting plasmids were designated as follows: LV-METTL3-RNAi (cat. no. 112185-1; shMETTL3-1), LV-METTL3-RNAi (cat. no. 112186-1; shMETTL3-2) and LV-METTL3-RNAi (cat. no. 112187-1; shMETTL3-3). The core targeting sequences (guide strand, 5'-3') were: shMETTL3-1, GAAGGA ACACTGCTTGGTTGG; shMETTL3-2, GAACCAACAGTC AACGAAAGA; and shMETTL3-3, GCCAAGGAACAGTCC ATTGTT. A non-targeting shRNA with the sequence 5'-TTC TCCGAACGTGTCACGT-3' (cat. no. CON313; Shanghai GeneChem Co., Ltd.) was used as a negative control (shNC). Seed-region BLAST analysis (nucleotides 2-8 of the guide strand) confirmed that these sequences specifically target METTL3 with no perfect matches to other known mouse genes.

Lentiviral particles were generated using a second-generation self-inactivating packaging system. Briefly, 293T cells (Chinese Academy of Sciences) were co-transfected with the GV493 vector plasmid (20 μg per 10 cm dish), the packaging plasmid pHelper 1.0 (15 μg; containing gag, pol and rev genes), and the envelope plasmid pHelper 2.0 (10 μg; encoding VSV-G), at a ratio of ~4:3:2. Transfection was performed at 37˚C for 6 h, after which the medium was replaced with fresh complete medium. Cells were further cultured at 37˚C for 48-72 h, and lentiviral supernatants were collected. Among the three shRNAs, shMETTL3-1 was selected for all functional experiments based on its validated knockdown efficiency.

To establish stable knockdown cell lines, 3T3-L1 cells at ~60% confluency were transduced with shMETTL3-1 or shNC lentivirus at a multiplicity of infection of 8 for 16 h, after which the virus-containing medium was replaced with fresh complete medium. At 48 h post-transduction, stably transduced cells were selected with 3 μg/ml puromycin for 24 h. Following selection, the puromycin concentration was reduced to 1 μg/ml for maintenance culture. Cells were used for subsequent experiments after stable knockdown was confirmed.

ITTs and GTTs. At the 16-week time point, metabolic phenotyping of the mice was performed using glucose and insulin tolerance tests. For the GTT, mice were subjected to a 12 h fast, followed by an intraperitoneal injection of D-glucose (2 g/kg body weight) prepared as a 400 mg/ml solution. Blood glucose levels were measured using blood collected from the tail vein using a glucose meter (Kefu Industrial Co., Ltd.) at 0, 15, 30, 60, 90 and 120 min after injection.

An ITT was conducted after a 3-day recovery period following the GTT. Mice were fasted for 4 h and then intraperitoneally injected with insulin at a dose of 0.75 U/kg body weight. Blood glucose concentrations were monitored at 0, 15, 30, 60, 90 and 120 min after insulin administration. All glucose measurements were recorded and subjected to statistical analysis.

Histological analysis and hematoxylin and eosin (H&E) staining. Mouse adipose tissue (eWAT and iWAT) samples were fixed with 4% paraformaldehyde at 4˚C for 2 h, then dehydrated through a graded ethanol series (70, 80, 95 and 100%), cleared in xylene and embedded in paraffin wax. The paraffin-embedded tissues were sectioned at 7 μm thickness using a microtome. For H&E staining, the sections were dewaxed in xylene and rehydrated through a descending ethanol series to distilled water. The sections were then stained with Harris hematoxylin solution (Beijing Solarbio Science & Technology Co., Ltd.) for 8 min at room temperature (25˚C), followed by washing in running tap water for 5 min to allow blueing. Subsequently, the sections were counterstained with eosin Y solution (0.5%, w/v) for 2 min at room temperature. After dehydration through graded ethanol and clearing in xylene, the sections were mounted with neutral balsam mounting medium. Images were captured using a light microscope (Olympus Corporation) at x200 magnification. For adipocyte size quantification, at least three randomly selected non-overlapping fields per section and six mice per group were analyzed using ImageJ software (version 1.54p; National Institutes of Health), and the cross-sectional area of adipocytes was measured.

Statistical analyses. Data are presented as mean ± SD. Normality and variance homogeneity were verified. For multi-group comparisons, one-way or repeated-measures ANOVA was applied as appropriate, followed by Tukey's post hoc test for all pairwise comparisons. For direct two-group comparisons, an unpaired two-tailed Student's t-test was used. All analyses were performed using GraphPad Prism 10 (Dotmatics). $P<0.05$ was considered statistically significant.

Results

LIC-A monomer in FJHQT increases METTL3 expression in adipogenic 3T3-L1 cells. To identify candidate compounds that regulate METTL3 expression and AT homeostasis, compounds from FJHQT were retrieved using the TCMSP, and molecular docking was performed against METTL3 (PDB ID: 5TEY) using Discovery Studio. LibDock was used to sort the docking scores into binding free energies and molecular affinities (Table SII) to select 16 drug-like monomers (Fig. S1).

The optimal non-cytotoxic treatment concentration for each monomer in adipogenic 3T3-L1 cells was first determined using MTT assays across a range of concentrations (Fig. 1A). The cells were then treated with each monomer at the selected concentrations for 48 h. Western blot analysis revealed that, among all candidates, LIC-A significantly upregulated METTL3 protein expression compared with other drug monomers and the DMSO control (Fig. 1B and C). Moreover, dot blotting and colorimetric assays showed that LIC-A treatment markedly increased global RNA m6A modification levels (Fig. 1D and E). Together, these results indicated that LIC-A enhanced METTL3-mediated m6A modification in 3T3-L1 preadipocytes.

LIC-A ameliorates TNF-α- and LPS-induced adipokine dysregulation and inflammatory responses in differentiating 3T3-L1 adipocytes. To explore the effects of LIC-A on adipocyte function, adipokine and inflammatory factor expression in TNF-α- or LPS-stimulated adipogenic 3T3-L1 adipocytes was examined. The optimal LIC-A concentration was first determined under acute TNF-α stimulation (Fig. 2A) and 8 μmol/l was used in all subsequent cotreatment experiments (Fig. 2B-H). Differentiated adipogenic 3T3-L1 cells were challenged with the obesity-mimicking cocktail and followed by TNF-α treatment. ELISA showed that LIC-A treatment could significantly enhance adiponectin secretion and inhibit leukin secretion (leptin and resistin) when compared with the group treated by TNF-α alone (Fig. 2B and C). LIC-A also inhibited the release of inflammatory cytokines, such as IL-6 and IL-1β, induced by TNF-α (Fig. 2D) and elevated expression of insulin-sensitizing genes (Fig. 2E). At the transcriptional level, LIC-A significantly promoted the expression of adiponectin mRNA while suppressing leptin and resistin mRNA compared with the TNF-α group (Fig. 2F). Consistent with these findings, LIC-A significantly decreased the mRNA and protein levels of TNF-α-induced inflammatory factors (Fig. 2G and H).

Whether LIC-A exerts similar regulatory effects under acute LPS stimulation was further evaluated. The optimal LIC-A concentration under LPS stimulation was determined (Fig. 2I) and this concentration was used consistently (6 μmol/l) in all subsequent co-treatment experiments (Fig. 2J-O). It was observed that LIC-A treatment notably ameliorated LPS-induced alterations in adipokine secretion and inflammatory cytokine production (Fig. 2J-L). Moreover, LIC-A regulated mRNA and protein expression of adipokines and inflammatory factors in a manner highly consistent with its effects under TNF-α stimulation (Fig. 2M-O). Together, these data indicated that LIC-A alleviated TNF-α- and LPS-induced dysregulation of adipokine expression and inflammatory responses in adipogenic 3T3-L1 cells.

METTL3 deficiency abolishes the effects of LIC-A on adipokine dysregulation and inflammatory responses in TNF-α- or LPS-stimulated adipogenic 3T3-L1 cells. Since METTL3 upregulation may mediate the effects of LIC-A on TNF-α- and LPS-induced adipokine dysregulation and inflammatory responses, METTL3 protein levels in adipogenic 3T3-L1 cells were examined. Acute stimulation with TNF-α or LPS markedly decreased METTL3 levels, whereas LIC-A treatment restored them (Fig. 3A). Next, adipogenic 3T3-L1 cells were transduced with a METTL3-knockdown lentivirus. Knockdown efficiency was confirmed at the protein and mRNA levels (Fig. 3B and C). ELISA revealed that, in response to acute TNF-α stimulation, METTL3 knockdown abolished the beneficial effects of LIC-A. This was supported by the lack of increase in adiponectin secretion, lack of a significant decrease in leptin and resistin expression and lack of an effect on the secreted levels of key proinflammatory cytokines in comparison to the empty vector group (Fig. 3D-F). In accordance with these changes, METTL3 knockdown blocked the LIC-A upregulation of adiponectin mRNA and the downregulation of leptin, resistin and proinflammatory factor transcripts (Fig. 3G and H). Whether LIC-A could ameliorate secretory dysfunction under LPS challenge in METTL3 deficient cells was also investigated.

ELISA confirmed that METTL3 knockdown abrogated the protective effects of LIC-A under LPS challenge, as shown by the persistently low adiponectin secretion alongside unabated levels of leptin, resistin and inflammatory mediators. Consistent with this profile, qPCR analysis further revealed a parallel failure in the transcriptional regulation of these key metabolic and inflammatory genes (Fig. 3I-M). Collectively, these results indicated that the ability of LIC-A to counteract TNF-α- and LPS-induced adipokine dysregulation and inflammation depends on its promotion of METTL3 expression.

LIC-A alleviates HFD-induced metabolic disorders and AT dysfunction in obese mice. To assess the *in vivo* anti-obesity effects of LIC-A, obesity was induced in C57BL/6J mice who were fed a HFD over a 12-week period. Experimental animals (4-16 weeks of age) were treated with LIC-A (60 mg/kg) by oral gavage (twice a week) (Fig. 4A). The body weight of the experimental group treated with LIC-A decreased compared with that of the HFD control group (Fig. 4B and C). These changes were associated with improved insulin sensitivity and glucose homeostasis (Fig. S2A and B) and reduced hyperglycemia and dyslipidemia (Fig. S2C). In addition, LIC-A efficiently attenuated WAT mass enlargement and impeded the pathological remodeling of this tissue (Fig. 4D and E).

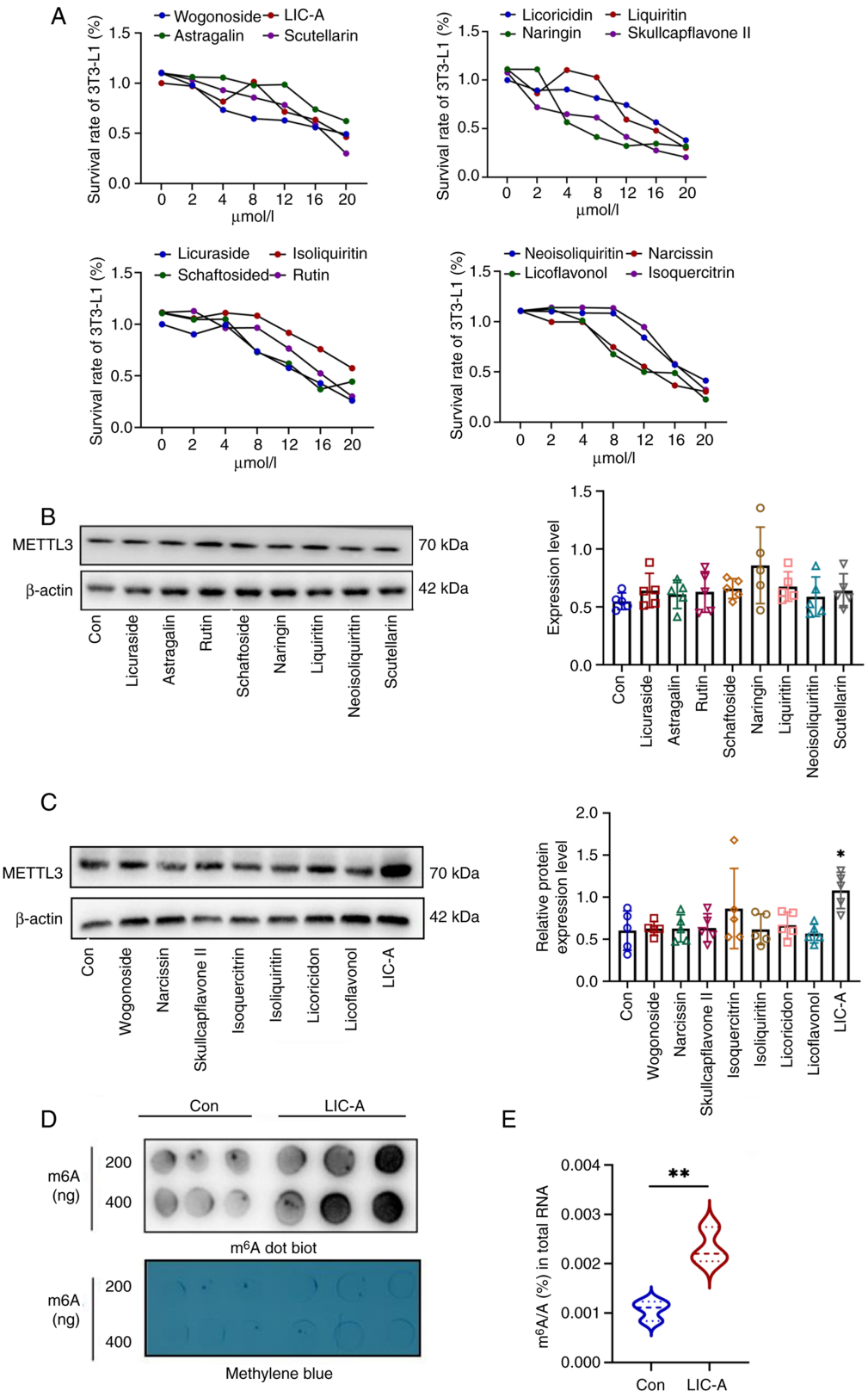

Figure 1. LIC-A monomer in FJHQT promotes METTL3 expression in adipogenic 3T3-L1 cells. (A) Viability of 3T3-L1 cells treated with the indicated drugs at various concentrations, as determined by MTT assay. (B) Western blot analysis of METTL3 protein expression in 3T3-L1 cells following treatment with individual compounds, with corresponding densitometric semi-quantification. (C) An independent western blot analysis of METTL3 protein expression in 3T3-L1 cells following treatment with individual compounds, with corresponding densitometric semi-quantification. (D) Global m^{6}A levels in mRNA from LIC-A-treated 3T3-L1 cells, measured by m^{6}A dot blot using an anti-m^{6}A antibody. (E) Quantitative analysis of global mRNA m^{6}A levels in LIC-A-treated cells using a colorimetric ELISA kit. For western blot analysis in (B) and (C), data are presented as mean ± SD from five independent experiments (n=3 per group), and statistical significance was determined by one-way ANOVA followed by Tukey's post hoc test for multi-group comparisons. For MTT assay (A), data are presented as mean ± SD from three independent experiments (n=3 per group), also analyzed by one-way ANOVA with Tukey's post hoc test. For m^{6}A dot blot in (D) and colorimetric ELISA in (E), which involve direct two-group comparisons, data are presented as mean ± SD from three independent experiments (n=3 per group) and were analyzed using unpaired two-tailed Student's t-test. *P<0.05, **P<0.01. FJHQT, Fangji-Huangqi Decoction; LIC-A, licoisoflavone A; METTL3, methyltransferase 3; m^{6}A, N^6-methyladenosine.

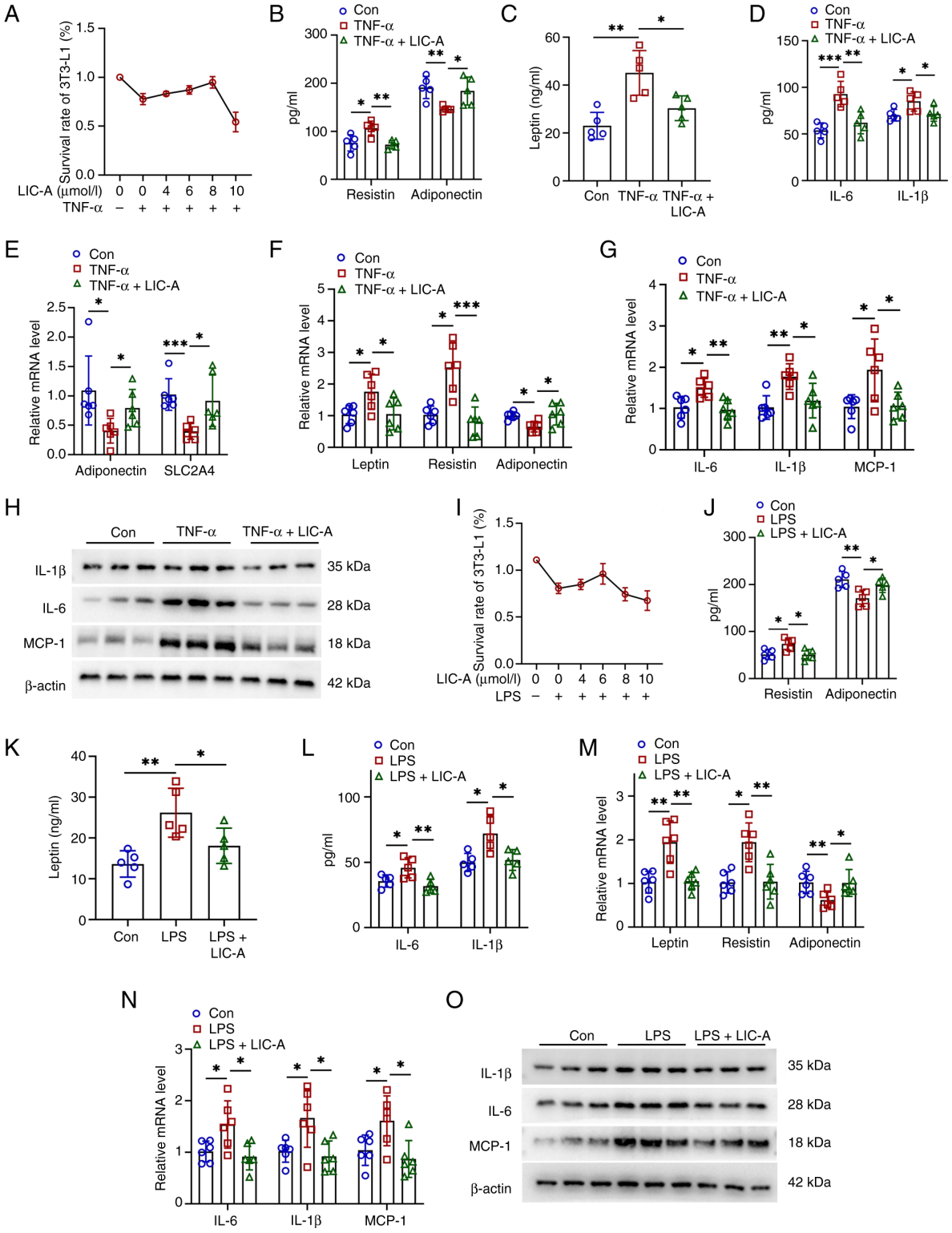

Figure 2. LIC-A ameliorates TNF-α- and LPS-induced adipokine dysregulation and inflammatory responses in differentiating 3T3-L1 adipocytes. (A) Determining optimal LIC-A concentration under TNF-α stimulation by MTT assay. (B-H) Differentiated 3T3-L1 adipocytes were stimulated with TNF-α (10 ng/ml) in the presence or absence of LIC-A (8 μmol/l) for the indicated periods. (B) ELISA measuring secreted levels of adiponectin and resistin. (C) ELISA measuring secreted levels of leptin. (D) ELISA measuring secreted levels of pro-inflammatory cytokines IL-6 and IL-1β. (E) Analyzing mRNA expression of insulin sensitivity genes by qPCR. (F) qPCR analysis of mRNA expression of adipokines (adiponectin, leptin and resistin). (G) qPCR analysis of mRNA expression of inflammatory cytokines (IL-6, IL-1β and MCP-1). (H) Detecting protein levels of inflammatory cytokines by western blotting. (I) Determining optimal LIC-A concentration under LPS stimulation by MTT assay. (J-O) Differentiated 3T3-L1 adipocytes were stimulated with LPS (100 ng/ml) in the presence or absence of LIC-A (6 μmol/l) for the indicated periods. (J) ELISA measuring secreted levels of adiponectin and resistin. (K) ELISA measuring secreted levels of leptin. (L) ELISA measuring secreted levels of IL-6 and IL-1β. (M) qPCR analysis of mRNA expression of adipokines (adiponectin, leptin and resistin). (N) qPCR analysis of mRNA expression of inflammatory cytokines (IL-6, IL-1β and MCP-1). (O) Detecting protein levels of inflammatory cytokines by western blotting. For western blot analysis, data are presented as mean ± SD from three independent experiments (n=3 per group). For MTT, ELISA and qPCR assays, data are presented as mean ± SD from five independent experiments (n=5 per group). Statistical significance was determined by one-way ANOVA followed by Tukey's post hoc test. *P<0.05, **P<0.01, ***P<0.001. Con, control; LIC-A, licoisoflavone A; LPS, lipopolysaccharides; METTL3, methyltransferase 3; qPCR, quantitative polymerase chain reaction; MCP-1, monocyte chemoattractant protein-1.

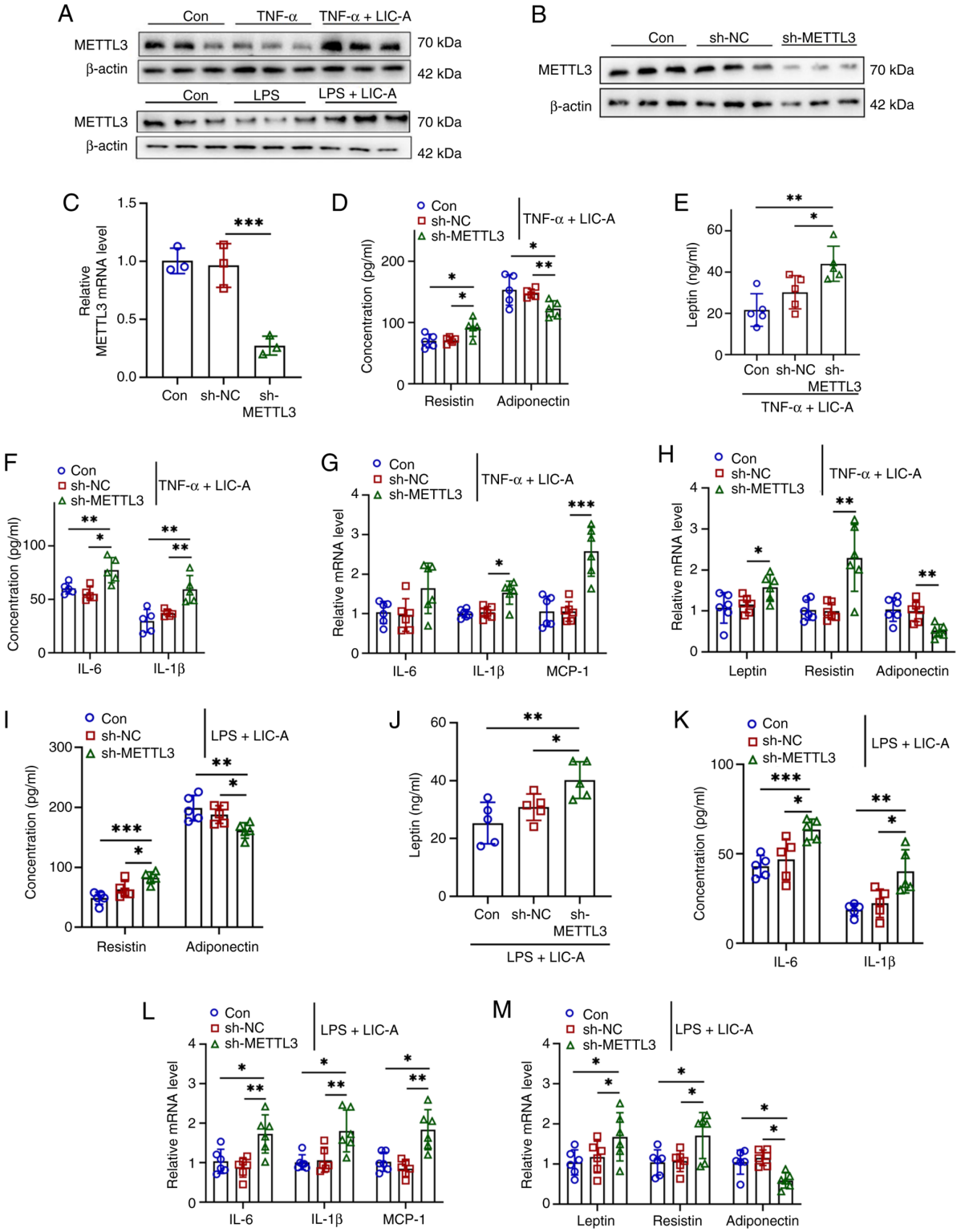

Figure 3. METTL3 deficiency abolishes the effects of LIC-A on adipokine dysregulation and inflammatory responses in TNF-α- or LPS-stimulated adipogenic 3T3-L1. (A) Western blot analysis of METTL3 protein expression during adipogenesis in 3T3-L1 cells under acute TNF-α or LPS stimulation. (B) Western blot analysis verifying the knockdown efficiency of METTL3 in adipogenic 3T3-L1 cells. (C) qPCR analysis verifying the knockdown efficiency of METTL3 in adipogenic 3T3-L1 cells. (D-H) METTL3-knockdown 3T3-L1 adipocytes were stimulated with TNF-α (10 ng/ml) in the presence or absence of LIC-A (8 μmol/l) for the indicated periods. (D) ELISA measuring secreted levels of adiponectin and resistin. (E) ELISA measuring secreted levels of leptin. (F) ELISA measuring secreted levels of pro-inflammatory cytokines IL-6 and IL-1β. (G) qPCR analysis of mRNA expression of inflammatory cytokines IL-6 and IL-1β. (H) qPCR analysis of mRNA expression of Adipoq, leptin, resistin and MCP-1. (I-M) METTL3-knockdown 3T3-L1 adipocytes were stimulated with LPS (100 ng/ml) in the presence or absence of LIC-A (6 μmol/l) for the indicated periods. (I) ELISA measuring secreted levels of adiponectin and resistin. (J) ELISA measuring secreted levels of leptin. (K) ELISA measuring secreted levels of IL-6 and IL-1β. (L) qPCR analysis of mRNA expression of inflammatory cytokines Il6, IL-1β and MCP-1. (M) qPCR analysis of mRNA expression of adipokines Adipoq, leptin and resistin. For western blot analysis data are presented as mean ± SD from three independent experiments (n=3 per group). For MTT, ELISA and qPCR assays, data are presented as mean ± SD from five independent experiments (n=5 per group). Statistical significance was determined by one-way ANOVA followed by Tukey's post hoc test. *P<0.05, **P<0.01, ***P<0.001. Con, control; LIC-A, licoisoflavone A; LPS, lipopolysaccharides; METTL3, methyltransferase 3; qPCR, quantitative polymerase chain reaction; MCP-1, monocyte chemoattractant protein-1; sh, short hairpin RNA; NC, negative control.

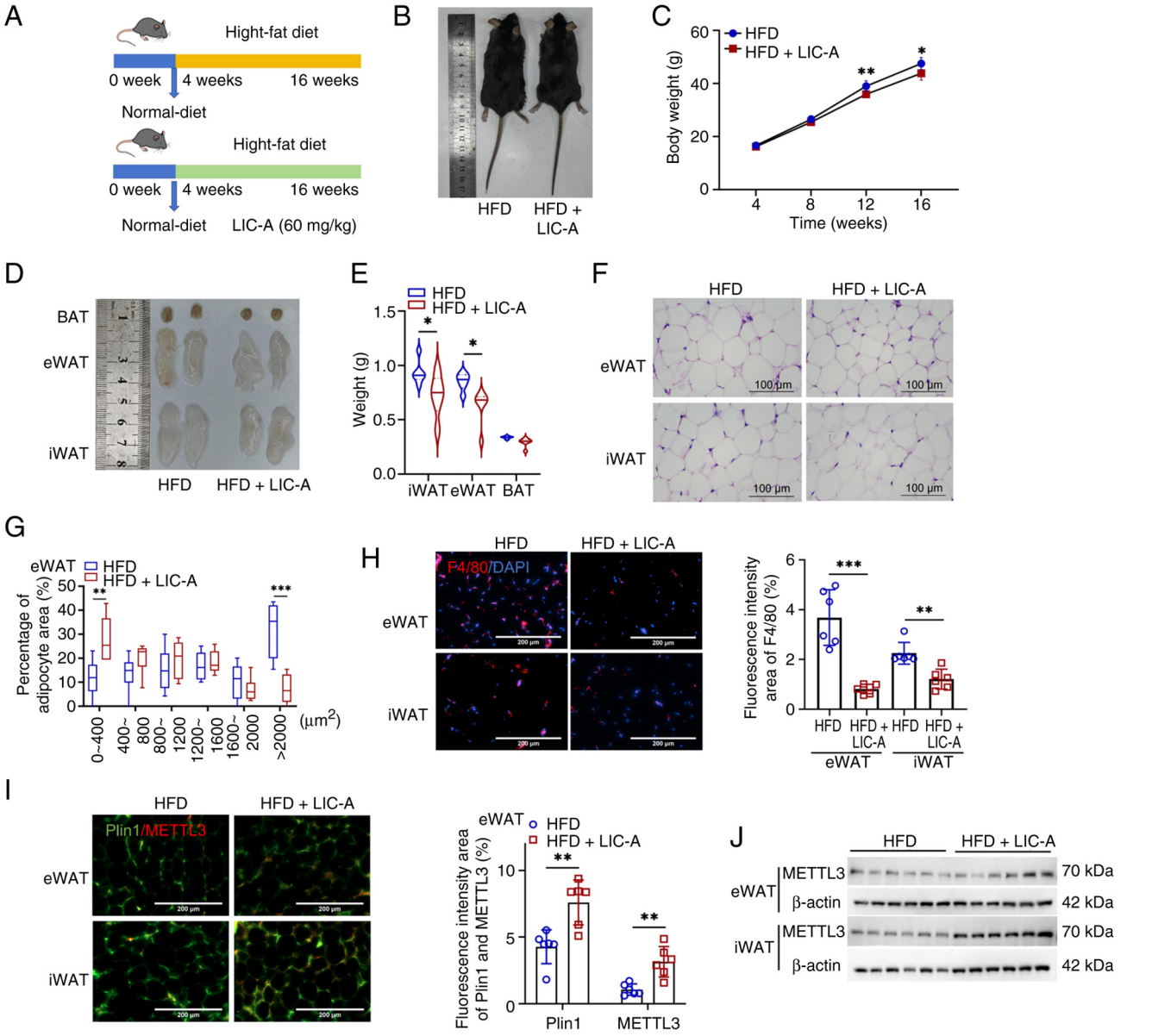

Figure 4. LIC-A alleviates HFD-induced metabolic disorders and AT dysfunction in obese mice. (A) Schematic of the HFD experimental strategy. (B) Representative gross morphology of mice after 16 weeks. (C) Monitoring of body weight changes. (D and E) Examination of eWAT morphology and weight. (F) Histological assessment of AT by hematoxylin and eosin staining. (G) Quantification of adipocyte size frequency distribution in eWAT. (H) Assessing macrophage infiltration by F4/80/DAPI immunofluorescence and quantitative analysis of inflammatory areas. (I) Analyzing METTL3 localization by Plin1/METTL3 immunofluorescence and quantitative analysis of METTL3-positive areas. (J) Detecting METTL3 protein levels in WAT by western blot. All data are presented as mean ± SD (n=6 mice per group for both HFD control and LIC-A treatment groups). Statistical significance was determined by one-way ANOVA followed by Tukey's post hoc test. ns, not significant; *P<0.05, **P<0.01, ***P<0.001. AT, adipose tissue; BAT, brown adipose tissue; Con, control; eWAT, epididymal white adipose tissue; HFD, high-fat diet; iWAT, inguinal white adipose tissue; LIC-A, licoisoflavone A; LPS, lipopolysaccharides; METTL3, methyltransferase 3.

A notable reduction in the size of adipocytes in the eWAT of LIC-A-treated animals was observed (Fig. 4F, 4G and S2D), which reflects the inhibition of adipocyte hypertrophy, a hallmark of dysfunctional eWAT in obesity.

Notably, LIC-A treatment markedly attenuated eWAT inflammation. Immunofluorescence staining for the macrophage marker F4/80 revealed a significant reduction in macrophage infiltration (quantified as F4/80-positive area) in the eWAT of LIC-A-treated mice compared with HFD controls (Fig. 4H). Consistently, the entire panel of adipokines showed a metabolically favorable shift. ELISA of eWAT homogenates further showed increased adiponectin levels and decreased levels of leptin, resistin and inflammatory factors. Furthermore, qPCR analysis of inflammatory gene expression at the transcript level confirmed the downregulation of proinflammatory genes (Fig. S2E-H).

Notably, LIC-A treatment also elevated METTL3 expression in the AT of mice, thereby recapitulating the *in vitro* findings and confirming that LIC-A promotes METTL3 expression in both physiological and experimental settings (Fig. 4I and J). Taken together, these results demonstrated that LIC-A supplementation effectively alleviated metabolic dysregulation and pathological AT changes in diet-induced obese mice, suggesting that the beneficial effects of LIC-A may

be mediated, at least in part, through METTL3 upregulation in AT.

Discussion

Obesity and its metabolic comorbidities are associated with dysregulated AT, which becomes pathologically remodeled and chronically inflamed and exhibits altered adipokine secretion (45-47). The present study identified LIC-A as a new upstream regulator of the RNA methyltransferase METTL3 and showed that LIC-A alleviated the metabolic disturbances associated with obesity by stimulating METTL3-mediated m^{6}A RNA methylation in the AT.

The present study combined virtual screening with functional validation. That is, molecular docking analysis, based on LibDock scores, identified LIC-A as exhibiting a favorable predicted binding affinity for METTL3 among the 16 candidate compounds screened from the FJHQT database. This prediction guided the selection of LIC-A for experimental validation. The *in vitro* experimental results confirmed the hypothesis derived from the docking analysis, demonstrating that LIC-A promoted METTL3 protein expression and induced m^{6}A modification. Furthermore, *in vivo* experimental data from HFD mice further demonstrated that LIC-A upregulated METTL3 expression in the AT; this observation was not limited to the cellular level but was also validated in a physiologically relevant context. Through these steps, beginning with computational predictions and validation of cellular mechanisms and culminating in metabolic assessments in whole animals, a relatively comprehensive body of evidence was established that supports the identification of LIC-A as a compound capable of regulating METTL3 expression.

Collectively, the data from the present study indicated that LIC-A upregulated METTL3 expression and increased global m^{6}A modification in adipogenic 3T3-L1 adipocytes, suggesting that LIC-A affects adipocyte metabolism through an epitranscriptomic mechanism. LIC-A treatment significantly reversed TNF-α- and LPS-induced deregulation of adipokines (leptin, adiponectin and resistin) and inhibited production of the pro-inflammatory cytokines. This protective effect was lost upon METTL3 knockdown, establishing an etiological link between anti-inflammatory and metabolic effects of LIC-A and METTL3. *In vivo*, LIC-A effectively improved systemic glucose homeostasis, insulin sensitivity and lipid profiles in HFD-fed C57BL/6J mice. These improvements were associated with decreased adipocyte hypertrophy, reduced macrophage infiltration and ameliorated inflammation in eWAT.

The findings from the present study align with accumulating evidence that METTL3 is a key regulator of AT plasticity and metabolic health (48). Previous studies have demonstrated that METTL3 participates in beige adipogenesis and enhances glycolytic gene expression through m^{6}A modification, thereby promoting energy expenditure and glucose tolerance (29,30). In the present study, a basis for this therapeutic approach was provided by identifying a natural compound that may enhance METTL3 expression.

Additionally, endocrine dysfunction in the AT may be the primary mechanism by which LIC-A exerts its anti-obesity effects. The restoration of adipokine homeostasis and suppression of AT inflammation noted in the present study may partly explain the observed improvements in insulin resistance and dyslipidemia, which are manifestations of systemic AT dysfunction. Notably, decreased levels of leptin and resistin, coupled with the elevated levels of adiponectin, indicated that the role of LIC-A in improving endocrine dysfunction in AT is crucial for maintaining metabolic homeostasis.

The following limitations of the present study merits mentioning. First, LIC-A was identified as a METTL3 enhancer by molecular docking and functional assays, but direct binding of LIC-A to METTL3 has yet to be confirmed by biophysical approaches. Although the docking analysis revealed a favorable predicted binding mode of LIC-A within the METTL3 active pocket, this *in silico* observation served as a hypothesis-generating tool rather than a direct measure of the physical interaction. The subsequent *in vitro* and *in vivo* data collectively support the functional modulation of METTL3 by LIC-A, but do not unequivocally establish a direct ligand-protein binding event. Second, the downstream targets of METTL3 that mediate the LIC-A-induced improvement in metabolism need to be explored further, as RNA-sequencing and m^{6}A-sequencing could detect the individual transcripts whose methylation and expression are regulated by LIC-A. Third, the translational relevance of the data from the present study warrants systematic evaluation, including validation in human cells, comprehensive pharmacokinetic and toxicological profiling, and rigorous clinical testing. These studies will collectively determine whether LIC-A, a natural METTL3 agonist, could serve as an effective therapy for treating obesity and its associated metabolic complications.

Based on the findings and limitations of the present study, we propose a general framework for developing LIC-A as a potential drug for the treatment of obesity and related metabolic diseases. First, at the molecular level, biophysical techniques should be used to definitively identify the precise molecular interaction sites between LIC-A and METTL3. Second, at the transcriptomic level, an integrated analysis of m6A sequencing and RNA-sequencing data from METTL3-deficient adipocytes is needed to systematically identify downstream m^{6}A-modified transcripts that mediate the metabolic benefits of LIC-A, thereby revealing the complete LIC-A/METTL3/m^{6}A target gene regulatory axis. Third, at the physiological level, tissue-specific METTL3 conditional knockout mice will be used (for example achieving adipocyte-specific METTL3 deficiency using AdipoqCre) to definitively determine whether the *in vivo* anti-obesity effects of LIC-A stem directly from its action on METTL3 in AT or involve effects in other metabolic organs. Fourth, at the translational medicine level, rigorous pharmacokinetic and toxicological evaluations must be conducted in preclinical models, followed by validation in human primary adipocytes, and ultimately through carefully designed clinical trials to comprehensively assess the safety, efficacy and therapeutic potential of LIC-A in humans. In summary, we aim to systematically establish a progressive research pathway from molecular mechanisms to clinical translation with the goal of rigorously validating the therapeutic potential of LIC-A.

In the present study, it was confirmed that LIC-A is a first-in-class, natural agonist of METTL3, which is promising therapeutically for both obesity and metabolic disorders. Reconciling LIC-A with METTL3-catalyzed m^{6}A methylation

offers a mechanistic basis for how TCM compounds can influence epigenomic composition and reverse metabolic imbalances. The future framework aforementioned, which encompasses everything from biophysical binding assays and transcriptomic analysis to validation in human cells and translational pharmacology, provides a clear roadmap for consolidating the preclinical potential of LIC-A and advancing its development toward clinical applications.

Acknowledgements

Not applicable.

Funding

This study was supported by the National Natural Sciences Foundation of China (grant no. 82370463), Natural Science Foundation of the Guangxi Zhuang Autonomous Region (grant no. 2024GXNSFAA010154), Guangdong Basic and Applied Basic Research Foundation (grant no. 2025A1515012522) and the China Postdoctoral Science Foundation (grant no. 2024M761313).

Availability of data and materials

The data generated in the present study may be requested from the corresponding author.

Authors' contributions

ST was responsible for data acquisition and analysis, adipose tissue examination and writing the original draft. XW was responsible for the formal statistical analysis and interpretation of all quantitative data (including ELISA, qPCR, GTT/ITT metabolic parameters and serum biochemical indices), and contributed to the methodological optimization and quality control of the *in vitro* and *in vivo* experimental protocols. ZW was responsible for data curation and validation, including the molecular docking screening, MTT assay data collection and quantitative analysis of ELISA and qPCR results. HT was responsible for investigation and supervision, including conducting the cell culture and adipogenic differentiation experiments, and overseeing the daily operations of the animal experiments. KY was responsible for conceptualization and design, project administration, and critical revision of the manuscript. XZ completed conceptualization and contributed to writing, reviewing, and editing the manuscript. ST and XW confirm the authenticity of all the raw data. All authors read and approved the final version of the manuscript.

Ethics approval and consent to participate

The animal experiments of the project met the requirements of animal welfare ethics and passed the animal welfare ethics investigation by IACUC of Guilin Medical University (approval no. GLMU-IACUC-202510137).

Patient consent for publication

Not applicable.

Competing interests

The authors declare that they have no competing interests.

References

1. Neeland IJ, Lim S, Tchernof A, Gastaldelli A, Rangaswami J, Ndumele CE, Powell-Wiley TM and Despres JP: Metabolic syndrome. Nat Rev Dis Primers 10: 77, 2024.
2. Wang J, Li L, Zhang Z, Zhang X, Zhu Y, Zhang C and Bi Y: Extracellular vesicles mediate the communication of adipose tissue with brain and promote cognitive impairment associated with insulin resistance. Cell Metab 34: 1264-1279 e8, 2022.
3. Tasali E, Pamidi S, Covassin N and Somers VK: Obstructive sleep apnea and cardiometabolic disease: Obesity, hypertension, and diabetes. Circ Res 137: 764-787, 2025.
4. Kawai T, Autieri MV and Scalia R: Adipose tissue inflammation and metabolic dysfunction in obesity. Am J Physiol Cell Physiol 320: C375-C391, 2021.
5. Marcelin G, Gautier EL and Clement K: Adipose tissue fibrosis in obesity: Etiology and challenges. Annu Rev Physiol 84: 135-155, 2022.
6. Xue Y, Zou H, Ruan Z, Chen X, Lai Y, Yao D, Ung COL and Hu H: Pharmacoeconomic evaluation of anti-obesity drugs for chronic weight management: A systematic review of literature. Front Endocrinol (Lausanne) 14: 1254398, 2023.
7. Astrup A, Carraro R, Finer N, Harper A, Kunesova M, Lean ME, Niskanen L, Rasmussen MF, Rissanen A, Rossner S, *et al*: Safety, tolerability and sustained weight loss over 2 years with the once-daily human GLP-1 analog, liraglutide. Int J Obes (Lond) 36: 843-854, 2012.
8. Silver HJ, Olson D, Mayfield D, Wright P, Nian H, Mashayekhi M, Koethe JR, Niswender KD, Luther JM and Brown NJ: Effect of the glucagon-like peptide-1 receptor agonist liraglutide, compared to caloric restriction, on appetite, dietary intake, body fat distribution and cardiometabolic biomarkers: A randomized trial in adults with obesity and prediabetes. Diabetes Obes Metab 25: 2340-2350, 2023.
9. McGowan B, Ciudin A, Baker JL, Busetto L, Dicker D, Fruhbeck G, Goossens GH, Monami M, Sbraccia P, Martinez-Tellez B, *et al*: A systematic review and meta-analysis of the efficacy and safety of pharmacological treatments for obesity in adults. Nat Med 31: 3317-3329, 2025.
10. Nauck MA, Petrie JR, Sesti G, Mannucci E, Courreges JP, Lindegaard ML, Jensen CB, Atkin SL; Study 1821 Investigators: A phase 2, randomized, dose-finding study of the novel once-weekly human glp-1 analog, semaglutide, compared with placebo and open-label liraglutide in patients with type 2 diabetes. Diabetes Care 39: 231-241, 2016.
11. Chen XY, Zhang J and Zhu JS: The role of m^6A RNA methylation in human cancer. Mol Cancer 18: 103, 2019.
12. Yue Y, Liu J and He C: RNA N6-methyladenosine methylation in post-transcriptional gene expression regulation. Genes Dev 29: 1343-1355, 2015.
13. Oerum S, Meynier V, Catala M and Tisne C: A comprehensive review of m6A/m6Am RNA methyltransferase structures. Nucleic Acids Res 49: 7239-7255, 2021.
14. Wang T, Li X, Tao Y, Wang X, Li L and Liu J: METTL3-mediated NDUFB5 m6A modification promotes cell migration and mitochondrial respiration to promote the wound healing of diabetic foot ulcer. J Transl Med 22: 643, 2024.
15. Hou X, Yang Y, Wang C, Huang Z, Zhang M, Yang J, Li N, Yang H, Yang L and Wu K: H3K36 methyltransferase SMYD2 affects cell proliferation and migration in Hirschsprung's disease by regulating METTL3. J Cell Physiol 239: e31402, 2024.
16. Yuan W, Ouyang S, Lv Q and Liao L: The effect of m6A methyltransferase METTL3 mediated TMEM30A regulation on tumor energy metabolism and cisplatin anti-tumor activity in oral squamous cell carcinoma. Life Sci 358: 123122, 2024.
17. Li Y, Wang J, Huang C, Shen M, Zhan H and Xu K: RNA N6-methyladenosine: A promising molecular target in metabolic diseases. Cell Biosci 10: 19, 2020.
18. Wang C, Tanizawa H, Hill C, Havas A, Zhang Q, Liao L, Hao X, Lei X, Wang L, Nie H, *et al*: METTL3-mediated chromatin contacts promote stress granule phase separation through metabolic reprogramming during senescence. Nat Commun 15: 5410, 2024.
19. Tuck MT: The formation of internal 6-methyladenine residues in eucaryotic messenger RNA. Int J Biochem 24: 379-386, 1992.

20. Qiu L, Jing Q, Li Y and Han J: RNA modification: Mechanisms and therapeutic targets. Mol Biomed 4: 25, 2023.
21. Liu J, Yue Y, Han D, Wang X, Fu Y, Zhang L, Jia G, Yu M, Lu Z, Deng X, *et al*: A METTL3-METTL14 complex mediates mammalian nuclear RNA N6-adenosine methylation. Nat Chem Biol 10: 93-95, 2014.
22. Jiang X, Liu B, Nie Z, Duan L, Xiong Q, Jin Z, Yang C and Chen Y: The role of m6A modification in the biological functions and diseases. Signal Transduct Target Ther 6: 74, 2021.
23. Wei J, Yu X, Yang L, Liu X, Gao B, Huang B, Dou X, Liu J, Zou Z, Cui XL, *et al*: FTO mediates LINE1 m^6A demethylation and chromatin regulation in mESCs and mouse development. Science 376: 968-973, 2022.
24. Wang X, Zhao BS, Roundtree IA, Lu Z, Han D, Ma H, Weng X, Chen K, Shi H and He C: N(6)-methyladenosine modulates messenger RNA translation efficiency. Cell 161: 1388-1399, 2015.
25. Shi H, Wang X, Lu Z, Zhao BS, Ma H, Hsu PJ, Liu C and He C: YTHDF3 facilitates translation and decay of N^6-methyladenosine-modified RNA. Cell Res 27: 315-328, 2017.
26. Zhang H, Lu W, Tang H, Chen A, Gao X, Zhu C and Zhang J: Novel insight of N6-methyladenosine in cardiovascular system. Medicina (Kaunas) 61: 222, 2025.
27. Zaccara S, Ries RJ and Jaffrey SR: Reading, writing and erasing mRNA methylation. Nat Rev Mol Cell Biol 20: 608-624, 2019.
28. Song B, Zeng Y, Cao Y, Zhang J, Xu C, Pan Y, Zhao X and Liu J: Emerging role of METTL3 in inflammatory diseases: Mechanisms and therapeutic applications. Front Immunol 14: 12216909, 2023.
29. Xie R, Yan S, Zhou X, Gao Y, Qian Y, Hou J, Chen Z, Lai K, Gao X and Wei S: Activation of METTL3 promotes white adipose tissue beiging and combats obesity. Diabetes 72: 1083-1094, 2023.
30. Li Y, Zhang Y, Zhang T, Ping X, Wang D, Chen Y, Yu J, Liu C, Liu Z, Zheng Y, *et al*: Rna M^6 a methylation regulates glycolysis of beige fat and contributes to systemic metabolic homeostasis. Adv Sci (Weinh) 10: e2300436, 2023.
31. Perez-Torres I, Castrejon-Tellez V, Soto ME, Rubio-Ruiz ME, Manzano-Pech L and Guarner-lans V: Oxidative stress, plant natural antioxidants, and obesity. Int J Mol Sci 22: 1786, 2021.
32. Li SZ, Zeng SL and Liu EH: Anti-obesity natural products and gut microbiota. Food Res Int 151: 110819, 2022.
33. Wang Y, Qi F, Li M, Xu Y, Dong L and Cai P: Traditional Chinese medicine modulates hypothalamic neuropeptides for appetite regulation: A comprehensive review. Biosci Trends 19: 281-295, 2025.
34. Wang Y, Ma Y, Ke Y, Jiang X, Liu J, Xiao Y, Zheng H, Wang C, Chen X and Shi M: Fangji Huangqi decoction ameliorates membranous nephropathy through the upregulation of BNIP3-mediated mitophagy. J Ethnopharmacol 324: 117734, 2024.
35. Li D, Yang C, Zhu JZ, Lopez E, Zhang T, Tong Q, Peng C and Lin LG: Berberine remodels adipose tissue to attenuate metabolic disorders by activating sirtuin 3. Acta Pharmacol Sin 43: 1285-1298, 2022.
36. Sen S, Tiwari AK, Binwal M, Israr M, Kumar A, Pathak N, Washimkar KR, Ratnasekhar CH, Mugale MN, Negi AS and Bawankule DU: Steroidal glycoside-rich extract of fenugreek seeds mitigates obesity-induced insulin resistance via attenuation of low-grade inflammation. Food Res Int 220: 117127, 2025.
37. Noh JW, Jun MS, Yang HK and Lee BC: Cellular and molecular mechanisms and effects of berberine on obesity-induced inflammation. Biomedicines 10: 1739, 2022.
38. Jang BC: Tetrandrine has anti-adipogenic effect on 3T3-L1 preadipocytes through the reduced expression and/or phosphorylation levels of C/EBP-α, PPAR-γ, FAS, perilipin A, and STAT-3. Biochem Biophys Res Commun 494: 422-423, 2017.
39. Zhu Y, Su Y, Zhang J, Zhang Y, Li Y, Han Y, Dong X, Li W and Li W: Astragaloside IV alleviates liver injury in type 2 diabetes due to promotion of AMPK/mTOR-mediated autophagy. Mol Med Rep 23: 437, 2021.
40. Wang L, Zheng W, Yang J, Ali A and Qin H: Mechanism of Astragalus membranaceus alleviating acquired hyperlipidemia induced by high-fat diet through regulating lipid metabolism. Nutrients 14: 954, 2022.
41. Kim HL, Lee SK, Min DE, Choi BK and Lee DR: Anti-Obesity Effects of a mixture of atractylodes macrocephala and amomum villosum extracts on 3T3-L1 adipocytes and high-fat diet-induced obesity in mice. Molecules 27: 906, 2022.
42. Lee HE, Yang G, Han SH, Lee JH, An TJ, Jang JK and Lee JY: Anti-obesity potential of Glycyrrhiza uralensis and licochalcone A through induction of adipocyte browning. Biochem Biophys Res Commun 503: 2117-2123, 2018.
43. Hong MK, Han Y, Park HJ, Shin MR, Roh SS and Kwon EY: The synergistic action of metformin and glycyrrhiza uralensis fischer extract alleviates metabolic disorders in mice with diet-induced obesity. Int J Mol Sci 24: 936, 2023.
44. Livak KJ and Schmittgen TD: Analysis of relative gene expression data using real-time quantitative PCR and the 2(-Delta Delta C(T)) method. Methods 25: 402-408, 2001.
45. Younossi ZM, Kalligeros M and Henry L: Epidemiology of metabolic dysfunction-associated steatotic liver disease. Clin Mol Hepatol 31(Suppl): S32-S50, 2025.
46. Miranda AMA, McAllan L, Mazzei G, Andrew I, Davies I, Ertugrul M, Kenkre J, Kudo H, Carrelha J, Patel B, *et al*: Scott, Selective remodelling of the adipose niche in obesity and weight loss. Nature 644: 769-779, 2025.
47. An SM, Cho SH and Yoon JC: Adipose tissue and metabolic health. Diabetes Metab J 47: 595-611, 2023.
48. Ronningen T, Dahl MB, Valderhaug TG, Cayir A, Keller M, Tonjes A, Bluher M and Bottcher Y: m6A regulators in human adipose tissue-depot-specificity and correlation with obesity. Front Endocrinol (Lausanne) 12: 778875, 2021.